Cellulose Nanocrystal Assisted Dual-modification of Starch and Subsequent Polyvinyl Alcohol Blends

Yuanyuan Xia, Guihua Yang, Jiachuan Chen, and Zhaoyun Lin*

A cellulose nanocrystal (CNC) based dual-modification was explored as a means to achieve better film properties. Starch was mixed with 0.5 wt% CNC followed by oxidation with NaClO, then esterified with CNC and vinyl acetate. The dual-modified starch showed an increased degree of substitution, disrupted morphology, and decreased crystallinity. A remarkable catalytic effect of CNC was found with 0.3 wt% CNC in esterification, where the degree of substitution was 2.7 times higher than that of dual-modified starch without CNC. The best modifying condition was selected as 0.3 wt% CNC and 7.0 wt% vinyl acetate. The film generated from dual-modified starch, polyvinyl alcohol (PVOH), and glycerol generated a smooth surface and compact structure. Moreover, the films based on dual-modified starch had improved transparency, thermal stability, and tensile strength compared to that of native starch or oxidized starch. The highest tensile strength of film was obtained at 25.7 MPa with 30 wt% PVOH. The film showed the highest water resistance with a contact angle of 113°.

Keywords: Cellulose nanocrystal; Composite film; Esterification; Oxidation; Starch

Contact information: State Key Laboratory of Biobased Material and Green Papermaking/Key Lab of Pulp and Paper Science and Technology of Education Ministry of China, Qilu University of Technology, Shandong Academy of Sciences, Ji'nan, Shangdong Province, P. R. China, 250353;
**Corresponding author: linzhaoyun123@126.com*

INTRODUCTION

With increasing environmental problems, sustainable and biodegradable materials have received extensive attention. The effective utilization of biomass is the most available approach to produce value-added and bio-based products. Starch is an abundant biological compound that can be used to alleviate the problem of plastic waste (Zamudio-Flores *et al.* 2015; Yang *et al.* 2017). Natural starch has limitations on its potential applications due to its low rigidity, highly hydrophilic character, and thermal decomposition. However, these limitations can be overcome by starch modifications, through chemical, physical, and enzymatic methods (Zhao *et al.* 2017; Li *et al.* 2018; Sun *et al.* 2018; Surendra *et al.* 2018).

Starch is an important biopolymer for preparing biodegradable films. Modified starch determines the films properties with their optimized performance. Moreover, the modification usually involves single modification and dual-modification with multiple reagents or combined procedures. Dual-modified starch can improve the properties and uses of starch (Hong *et al.* 2018). When used as a binder, oxidized esterified starch improves the toughness of the composite more than single-modified starch (Chen *et al.* 2018). Oxidized-esterified starch has been observed to have lower crystallinity and better compatibility with alkalized fiber in the starch composite than native starch and single-modified starch (Zhao *et al.* 2017; Chen *et al.* 2018). A film of oxidized-acetylated banana starch was observed to improve the elastic modulus value and water vapor permeability

due to the introduction of ester groups (Zamudio-Flores *et al.* 2009). Oxidized and acid-modified starch has a high content of carbonyl and carboxyl groups, and it shows high water vapor permeability, tensile strength, stiffness, and low elongation in films (Biduski *et al.* 2017). Dual-modified starch shows additional dual or multiple performance, including hydrophilicity, adhesivity, swelling power, and compatibility (Xiao *et al.* 2012; Ashogbon and Akintayo 2014; Zhao *et al.* 2017). Therefore, double chemically modified starches have shown excellent performance that diversifies the application of starch films.

However, it is not sufficient to improve the properties of the film by improving the properties of starch solely. Various plasticizers and fillers have been used to reinforce the performance of starch-based films (Ravindra *et al.* 2019), for example, nanofillers. Cellulose nanofibers can be used as reinforcing agents due to their high aspect ratio, crystalline nature, and high mechanical strength (Vigneshwaran *et al.* 2011). Thermoplastic starch films fabricated with bamboo cellulose nanofibrils as reinforcing agent and glycerol plasticizer show high transparency and mechanical properties (Sasiprapa *et al.* 2019). However, the good performance of biopolymer films strongly depends on uniform distribution of nanofillers, which is a major challenge (Vigneshwaran *et al.* 2011). It has been proposed that cellulose nanocrystals (CNC) could penetrate into swelled starch granules due to their nano-size and needle-like structure, and then promote the penetration of oxidizer into starch (Liu *et al.* 2017). The oxidized starch is generated in the form of "CNC-oxidized starch". The application of CNC in starch modification and their application in films needs more in-depth work.

In this study, corn starch was modified with sodium hypochlorite and vinyl acetate, and CNC was used as catalyst. To understand the function of CNC in modifying starch, the effect of CNC dosage on the starch degree of substitution was investigated. The crystal structures and morphologies of native starch, single-modified starch, and dual-modified starch were compared. Consequently, the modified starch was blended with polyvinyl alcohol (PVOH) and glycerol (GL) to prepare starch-based films by a solution casting method. The film-forming ability of dual-modified starch was further investigated through optical properties, thermal properties, morphology, mechanical properties, and water resistance. The research introduced a new approach for incorporating CNC into starch and starch modification. The objective of this work was to prepare dual-modified starch with CNC serving as a green enabling component and to investigate its film-forming ability. The novelty of this research was the application of CNC for dual-modification of starch and the subsequent application in polyvinyl alcohol/glycerol blends.

EXPERIMENTAL

Materials

Cellulose nanocrystals with average length of 200 nm were made by acid hydrolysis (Sun *et al.* 2016) and stored at 4 °C. Corn starch powder with a gelatinization temperature of 45 °C was purchased from Macklin Biochemical Co., Ltd. (Shanghai, China). Analytical grade sodium hypochlorite with 10% active chlorine was obtained from Sigma-Aldrich (Tianjin, China). Analytical grade vinyl acetate (VAC) with the concentration of 99.5% was obtained from Sinopharm Chemical Co., Ltd. (Shanghai, China). Polyvinyl alcohol (PVOH with an alcoholysis degree of 97.5 to 99.0%), glycerol (GL), concentrated HCl and NaOH were all analytical reagents and purchased from Aladdin Reagent Co., Ltd. (Shanghai, China).

Methods

Preparation of oxidized-acetylated starch (OACS)

Starch was dissolved in distilled water at a concentration of 30 wt% in a water bath at 50 °C. Next, 0.5 wt% CNC (relative to dry starch) was added into the solution and mixed for 60 min in a water bath at 50 °C. Sodium hypochlorite with 8.0 wt% effective chlorine (relative to dry starch) was added as an oxidizer. The pH of the mixture was maintained at 9.0 by adding 0.1 M HCl and 0.1 M NaOH. After 4 h, 0.1 to 3.0 wt% CNC (relative to dry starch) was added and mixed for 60 min, and then 7.0 wt% vinyl acetate (relative to dry starch) was slowly added for esterification. The pH of the mixture was maintained at neutral, and this reaction was terminated after 2.5 h. Finally, the product was settled at room temperature for 2 h, filtered, washed with water and ethanol, and dried in a vacuum oven at 45 °C.

To investigate the function of CNC in the modifying process, three sets of control experiments were performed. In the first set of experiments, the oxidation and dual-modification were processed with CNC in the absence of starch. The dispersed CNC mixture with a concentration of 0.15 wt% was oxidized by NaClO (8.0 wt% effective chlorine, relative to dry CNC) for 4 h in a water bath at 50 °C; the dual-modification was processed followed by oxidation with 3.0 wt% vinyl acetate at 75 °C. The CNC specimens treated with oxidation and dual-modification were separately settled at room temperature for 2 h, filtered, washed with water and ethanol, and dried in vacuum oven at 45 °C. In the second set of experiments, starch was oxidized under the experimental conditions stated above with 8.0 wt% NaClO and 0.5 wt% CNC, and then esterified with various dosage of vinyl acetate (1.0 to 10.0 wt%, named as OACS without CNC). In the third set of experiments, starch was oxidized under the experimental conditions stated above with 8.0 wt% NaClO and 0.5 wt% CNC, and the reaction was terminated after 4 h by mixing with sodium thiosulfate (named as oxidized starch, OS).

Preparation of oxidized-acetylated starch (OACS)/PVOH/GL film

The oxidized-acetylated starch was dissolved in distilled water at a concentration of 10 wt% and mixed for 1 h at 50 °C. Next, 40 wt% PVOH and 25 wt% GL (relative to dry starch) were gradually added and mixed for 2 h at 90 °C. After ultrasonication, the film-forming solution was transferred to a PTFE (polytetrafluoroethylene) mold with a fixed quantity of 0.15 g/cm^2, peeling off the film after air drying and conditioning it at 50% RH for 12 h.

Measurements

Modified starch was characterized by a Fourier transform infrared spectroscopy (FT-IR; Vertex70, Bruker, Karlsruhe, Germany) with a resolution of 4 cm^{-1} ranging from 400 cm^{-1} to 4000 cm^{-1}. The crystalline structure was analyzed with an x-ray diffractometer (XRD; D8-ADVANCE, Bruker, Karlsruhe, Germany) at room temperature in the ranges of 2θ = 10 to 40°. The carboxyl content of oxidized starch was determined as previously described (Dang *et al.* 2018). The degree of substitute (DS) of starch was determined according to the modified procedure (Han *et al.* 2012). The morphology of starch was observed on a scanning electron microscope (SEM; Quanta 2000, ThermoFisher, Waltham, MA, USA) at an accelerating voltage of 15 kV.

The thickness of 10 films was tested with a thickness meter (LT/ZH-4, Jiangsu, China), and the average values were calculated. The optical properties of the composite films were tested by a UV-Vis spectrometer (Cary 5000, Agilent, Palo Alto, USA) in the wavelength range from 200 nm to 800 nm. All samples were cut to 50 × 50 mm for inserting into a spectrophotometer cell after receiving absorption coefficients. The refractive indices (n_D) of starch solution (10 wt%) and PVOH/GL (40/25, mass ratio) were tested using a Digital Abbe refractor (WAY-2S, INESA, Shanghai, China). To observe the fracture surface without destruction, all films were fractured under liquid nitrogen. Static state contact angles of films were analyzed by a contact angle goniometer (JC2000C1, POWEREACH, Shanghai, China) with 5 μL deionized water. Five different positions were detected for each film. The mechanical properties of composite films were tested with an Instron 5900 testing machine (Gotech testing machines CO., LTD, Dongguan, China) at a fixed tensile speed of 50 mm/min, with films cut to 70 × 10 mm.

RESULTS AND DISCUSSION

Fourier Transform Infrared (FTIR) Spectroscopy of Starch

The FT-IR spectra of corn starch (CS), oxidized starch (OS), oxidized-acetylated starch with CNC (OACS) and oxidized-acetylated starch without CNC are shown in Fig. 1. Corn starch showed strong peaks in the range of 3000 cm^{-1} and 3600 cm^{-1}, which corresponded to -OH stretching. The band located at 2931 cm^{-1} was related to -CH stretching. The bands of 1646 cm^{-1} and 1458 cm^{-1} were assigned to -OH and -CH bending, respectively. The bands at 1017 to 1368 cm^{-1} were assigned to C-C group, C-O group, and C-O-C group (Lin *et al.* 2013). Oxidized starch showed a new peak at 1719 cm^{-1}, which was attributed to the introduction of a carboxyl group (Gutiérrez and Alvarez 2016) and indicated successful oxidation.

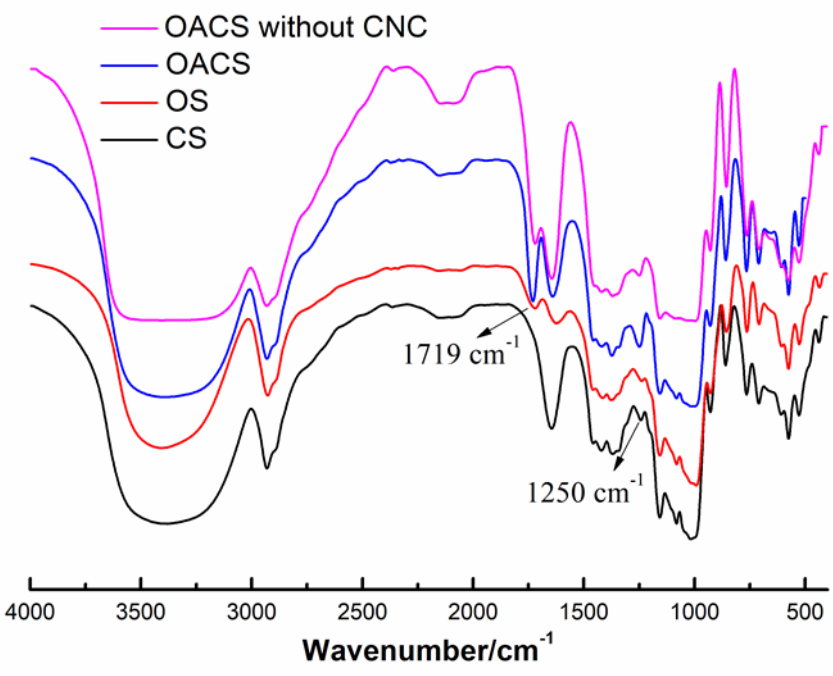

Fig. 1. FT-IR spectra of corn starch (CS), oxidized starch (OS), and oxidized-acetylated starch (OACS)

To analyze the function of CNC in esterification, a control sample of OACS (OACS without CNC, 7.0 wt% vinyl acetate) was prepared in the second set of experiments. The OACS showed increased peak intensity at 1719 cm^{-1} and 1250 cm^{-1} due to the C=O and C-O stretching vibration of carbonyl. Moreover, the OACS showed stronger peak intensity at 1719 cm^{-1} than the control OACS (OACS without CNC). Therefore, the acetyl group was introduced, and the addition of CNC improved the esterification of oxidized starch.

Degree of Substitution (DS)

The DS of OACS was investigated by changing the addition of vinyl acetate (VAC) and CNC in esterification, as shown in Table 1. Previously, the effect of CNC addition on oxidizing degree was investigated, with the highest carboxyl content attained with 0.5 wt% CNC (Xia *et al.* 2018). In this dual-modification process, oxidized starch was selected with the highest oxidation level. Oxidized starch with a low carboxyl group ratio (< 0.04%) is easily esterified due to its partial depolymerization and weak structure; whereas, oxidized starch with a high carboxyl group ratio (> 0.40%) shows low susceptibility to acetylation because hydroxyl groups have low availability and accessibility (Mo *et al.* 2014; Pietrzyk *et al.* 2014). The oxidized starch with 0.5 wt% CNC had a relatively high carboxyl content at 1.10%, which was bad for esterification.

As shown in Table 1, the DS of control OACS (in the second set of experiments) increased from 0.024 to 0.058 with increasing dosage of vinyl acetate up to 7.0 wt.%. However, with 7.0 wt% vinyl acetate, the DS of OACS was greatly increased by adding CNC. The highest DS was attained at 0.214 containing 0.3 wt% CNC. The DS of acetylated starch is classified as low (< 0.1) and medium (0.1 to 1.0) for different applications (Halal *et al.* 2015). Hence, the addition of CNC improved the dual-modified starch with a medium DS, and it was beneficial to esterification even at high carboxyl ratio. Based on a previous study (Liu *et al.* 2017), the improved DS may be ascribed to the penetration of CNC into the swelled starch granules, which enlarged the specific surface area between starch and vinyl acetate. Nevertheless, excessive addition of CNC hinders penetration because of the aggregation of CNC on the starch surface. Hence, the esterification reaction conditions were set as 7 wt-% vinyl acetate and 0.3 wt% CNC.

The changes of CNC were studied to explore its function in the dual-modification of starch. The carboxyl content of CNC after treating with NaClO was tested, in which CNC consumed the same volume of NaOH with untreated CNC. The DS of CNC treated with NaClO and vinyl acetate was also tested, and it showed a result of zero. Therefore, it was concluded that there were no carboxyl groups and acetyl groups on CNC after treating with NaClO and vinyl acetate in the first control experiment.

Table 1. Degree of Substitution (DS) of OACS with Different Addition of Vinyl Acetate (VAC) and CNC

Addition of VAC/wt.%	DS	Addition of CNC/wt%	DS
1.0	0.024±0.001	0.1	0.122±0.011
3.0	0.039±0.003	0.3	0.214±0.020
5.0	0.046±0.004	0.5	0.196±0.015
7.0	0.058±0.006	1.0	0.158±0.016
8.0	0.055±0.005	2.0	0.140±0.012
10.0	0.055±0.005	3.0	0.069±0.005

Crystal Structure of Starch

As shown in Fig. 2, the native corn starch showed strong peaks at 2θ =15.1°, 17.2°, 19.2°, and 23.1°, which were indication of typical A-type crystalline structure (Zavareze *et al.* 2012). The OS and OACS showed the same typical peaks, which indicated the unchanged crystal structure. Oxidation mainly occurred in the amorphous region of starch (Diop *et al.* 2011; Halal *et al.* 2015), and increased relative crystallinity of starch from 50.01% (native starch) to 56.64% (OS). The OACS showed the weakest peak intensity among native starch and OS. During esterification, some hydroxyl groups were replaced by acetyl groups, which led to reduced formation of inter- and intra-molecular hydrogen bonds and partial destruction of the ordered crystal structure (Zhang *et al.* 2009). Therefore, the amorphous region and crystalline region of starch were all affected, and its crystallinity was decreased. Moreover, the CNC resulted in OACS with a lower crystallinity (30.70%) than the control OACS (33.40%), implying that OACS had severe structural damage.

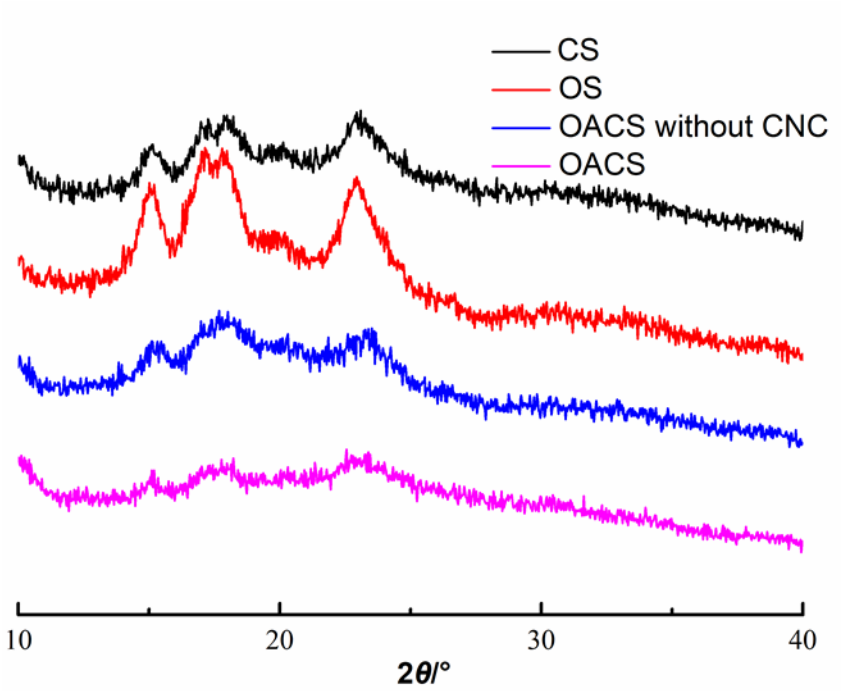

Fig. 2. X-ray spectra of corn starch (CS), oxidized starch (OS) and oxidized-acetylated starch with CNC (OACS) and oxidized-acetylated starch without CNC

Morphology of Starch

The scanning electron micrographs of native starch, oxidized starch, and oxidized-acetylated starch granules are shown in Fig. 3. Native starch had a smooth surface and polyhedral shape (Fig. 3A). The oxidative reaction between starch and oxidizer led to chain scission (Zhao *et al.* 2017) and the disrupted structure of starch. As shown in Fig. 3B, the surface of oxidized starch was rough and covered with tiny fragments. The oxidizer corroded and broke the structure of starch. After oxidation and esterification (Fig. 3C), the surface of starch showed a higher disintegration, with some agglomerates. Oxidation and esterification preferentially attack the amorphous region of starch (Diop *et al.* 2011), leading to the removal of these regions and rupture of the starch granules.

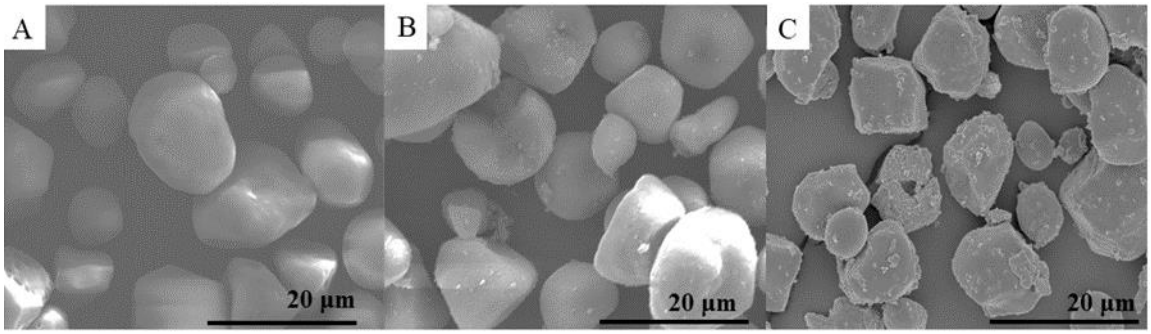

Fig. 3. Scanning electron micrographs of (A) corn starch (CS), (B) oxidized starch (OS) and (C) oxidized-acetylated starch (OACS)

Optical Properties of Films

The visible light transparency of all films fabricated by starch and PVOH/GL were determined by UV-Visible spectroscopy. The light absorption coefficient was obtained at a fixed wavelength λ of 600 nm (Aulin *et al.* 2013), and transparency was calculated as follows,

$$T = t/A_{600} \quad (1)$$

where A_{600} is the adsorption coefficient (λ = 600 nm) and t is the film thickness. Native corn starch-based films showed a low transparency at 56.49%, whereas the incorporation of modified starch with PVOH/GL led to improved optical transparency. The OACS-based film exhibited higher transparency than OS-based film. The OACS containing 0.3 wt.% CNC made the film with the highest transparency. The introduction of acetyl group into OACS improved the dispersibility, and the disrupted structure facilitated their compatibility with PVOH/GL matrix. In addition, the low crystallinity of OACS indicated low crystal boundaries and less scattering (Aulin *et al.* 2013; Sasiprapa *et al.* 2019). The refractive index of corn starch was 1.55, the refractive indices of OACS with 0.1 wt%~0.5 wt% CNC were 1.51, 1.50 and 1.50 respectively. So the difference of refractive indices between OACS and PVOH/GL (n_D = 1.47) was reduced. All of these factors contributed to the high transparency of films.

Table 2. Transparency of Films with CS, Modified Starch Containing Various CNC Additions

Films	CS	OS	OACS	OACS	OACS
Addition of CNC (wt.%)	0	0.5	0.1	0.3	0.5
Transparency (%)	56.49± 5.16	65.61± 6.91	70.12± 6.99	75.89± 7.01	75.86± 7.11

Morphology of Films

The microstructure of the surface and cross-sectional surface of starch-based films were observed with SEM (Fig. 4), revealing the dispersity of starch in PVOH/GL. The corn starch-based film had a heterogeneous surface and discrete structure; some starch granules kept their shape in the films. The linked cross-sectional image showed a profile with many fragments and indicated a bad miscibility between starch, PVOH, and GL (as shown in Fig. 4a, a'). However, the modified starch-based films had more a homogeneous and continuous surface compared with the native starch-based film.

The oxidized starch-based film showed a homogeneous surface and cross-sectional surface (Fig. 4b, b') due to the depolymerization of oxidized starch molecule and subsequent high penetration of plasticizer molecules into the starch chains (Biduski *et al.* 2017). Although the interaction between these components was improved, the film still showed little fragments in the surface and cross section. The dual-modified starch led to a smoother surface and more homogenized structure of the composite films (shown in Fig. 4c, c'). It was clear that the dual-modification disrupted the crystal structure of oxidized starch. The molecular structure of OACS was relatively more dispersed and generated a compact structure with PVOH/GL.

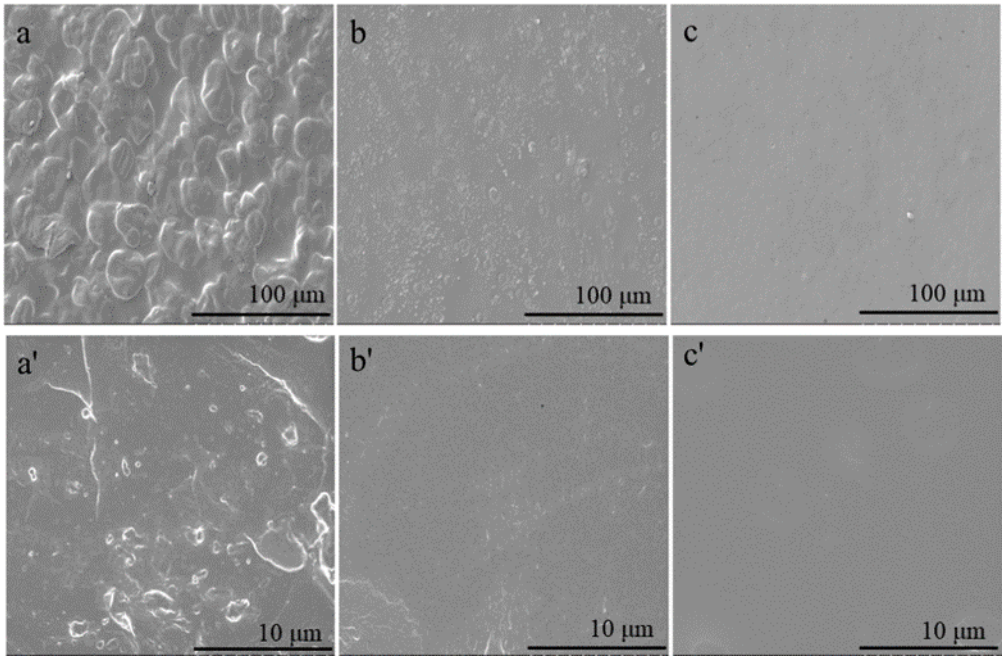

Fig. 4. SEM micrographs of the surfaces and fractures of the composite film fabricated by (a, a') corn starch (CS), (b, b') oxidized starch (OS) and (c, c') oxidized-acetylated starch (OACS)

Thermal Properties of Films

The thermal stability of films was analyzed by TGA, and the thermogravimetric curve (TG) and derivative thermogravimetric curves (DTG) are displayed in Fig. 5. The thermal stability of PVOH/GL was tested to identify the origin of the different degradation steps; it showed two main degradation peaks at 308 °C and 480 °C for GL and PVOH, respectively. All films showed three main stages of decomposition, the first degradation took place in the region of 35 to 120 °C, which corresponded to the dehydration of water molecules. The sample mainly degraded in the region of 210 to 385 °C and showed the main weight loss. The CS-based film showed a higher residual weight percentage compared with PVOH/GL. The second degradation peak at 198 °C was assigned to the degradation of corn starch. However, the second degradation peak of OS-based film and OACS-based film on the DTG curves shifted to a higher temperature at about 230 °C, indicating an improved thermal stability of starch caused by the introduction of the carboxyl and acetyl groups into starch. All starch-based films showed weak degradation peaks at 300 °C and bare peak at 480 °C, which were attributed to the formation of hydrogen bond between starch and PVOH.

Mechanical Properties

Figure 6a shows the mechanical properties of the composite film fabricated by various starches. The native corn starch had poor interfacial adhesion, and phase separation easily occurred between starch, PVOH, and GL (Haafiz *et al.* 2013; Ahmet 2016; Almasi 2016). Thus, centers of stress concentration (granular aggregates) were easily formed, and the effective stress transfer in the corn starch-based film was easily broken. All these resulted in a low tensile stress and high tensile strain with corn starch-based film. The introduction of carboxyl groups in oxidized starch produced hydrogen bridges with the hydroxyl groups; the hydrogen bonds also provided improved structural integrity in the polymer matrix (Zhang *et al.* 2013).

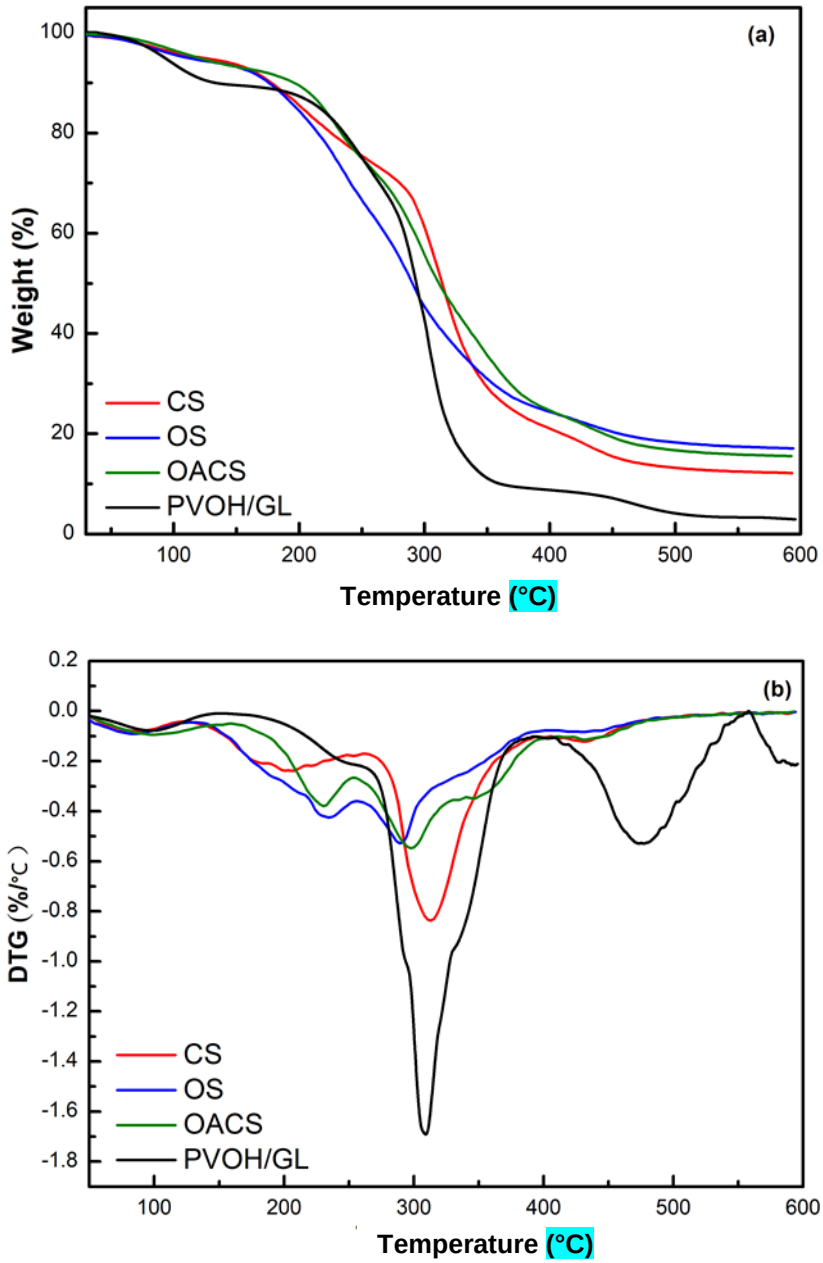

Fig. 5. TGA and DTG curves of composite films with native starch and modified starch

The penetration of CNC into starch formed "CNC-starch" composite, and then formed "CNC-oxidized starch" after the oxidation. The oxidized starch possessed good mechanical properties due to the incorporation of CNC with high crystalline and high stress. The OS-based film showed an improved tensile stress and reduced tensile strain, which was consistent with a previous study (Biduski *et al.* 2017). However, the introduction of acetyl groups led to the development of a more resistant matrix by reinforced hydrogen bond interaction between aligned polymeric chains (López *et al.* 2011). In addition, the increasing incorporation of CNC continuously improved the mechanical properties of starch. Therefore, oxidized-acetylated starch led to higher tensile stress than that of oxidized starch-based film.

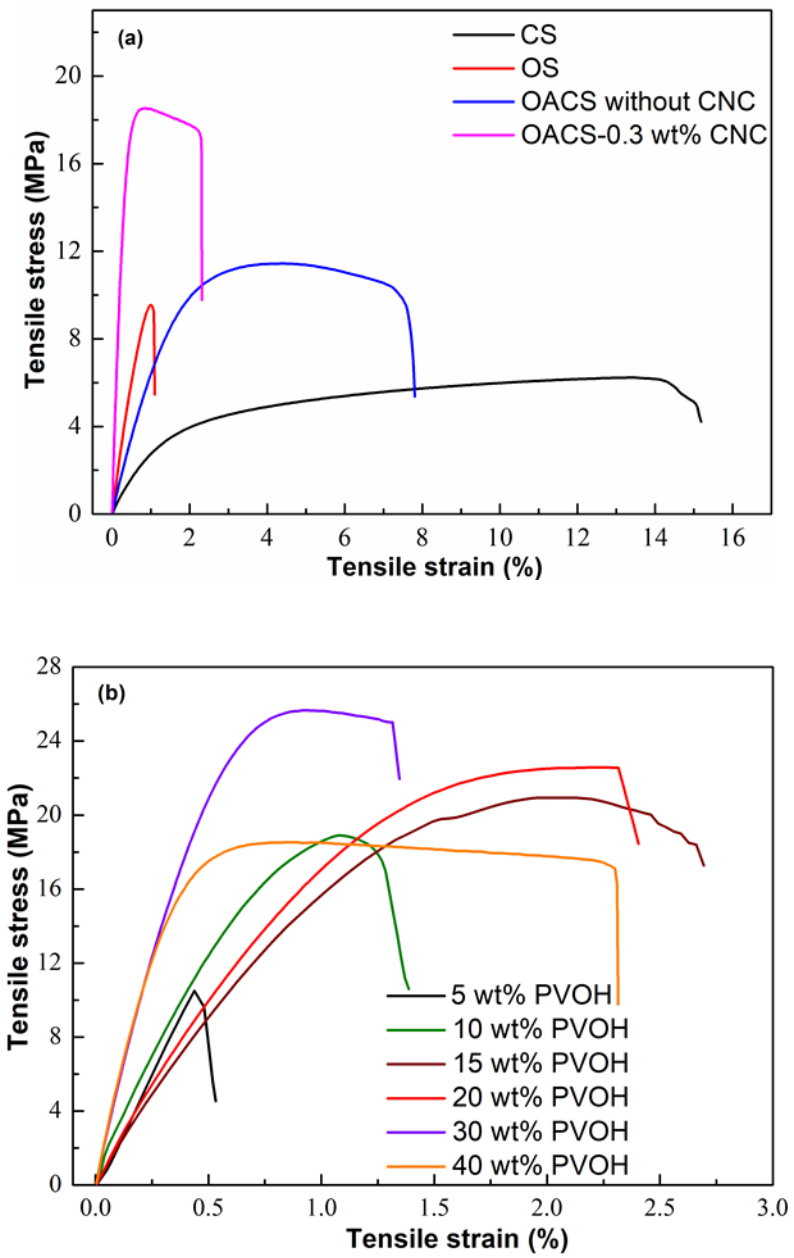

Fig. 6. The mechanical properties of composite films with various starch (a) and various content of PVOH.

The mass ratio of PVOH/GL was fixed at 1.6, and the effect of PVOH content on film mechanical properties is shown in Fig. 6b. The number of hydrogen bonds between starch and PVOH, and hydrogen bonds between starch, PVOH and GL increased with the increasing the content of PVOH and GL first. The tensile strength of films was increased by 25.7 MPa with 30 wt% PVOH. However, the increasing hydrogen bonding between starch and PVOH could restrain the molecular movement and processability. As a plasticizer, increasing addition of GL reduced the strong interactions by generating new hydrogen bonds with starch and PVOH, which left more free volume (Yan *et al.* 2012; Xu *et al.* 2016) and modified the films with a flexible material. Consequently, the tensile stress of film was decreased when PVOH content exceeded 30 wt%, but its tensile strain was improved. Young's modulus of composite film had the highest value with 30 wt% PVOH at 2500.8 MPa.

Table 3. Mechanical Properties of Composite Films as a Function of PVOH Content

PVOH dosage (wt%)	Stress (MPa)	Strain (%)	Young's module (MPa)
5	10.5±1.2	0.5±0.1	2259.4±120.5
10	18.9±1.5	1.4±0.3	1650.0±120.5
15	20.9±1.3	2.7±0.2	1782.3±99.3
20	22.6±1.2	2.4±0.3	1984.7±233.4
30	25.7±1.9	1.3±0.1	2500.8±190.5
40	18.5±1.4	2.3±0.2	1625.1±104.3

Hydrophobicity of Films

Figure 7 shows the contact angle of OACS-based film, in which OACS was modified along with various additions of CNC in esterification. The contact angle is used to determine the hydrophobicity of the film surface.

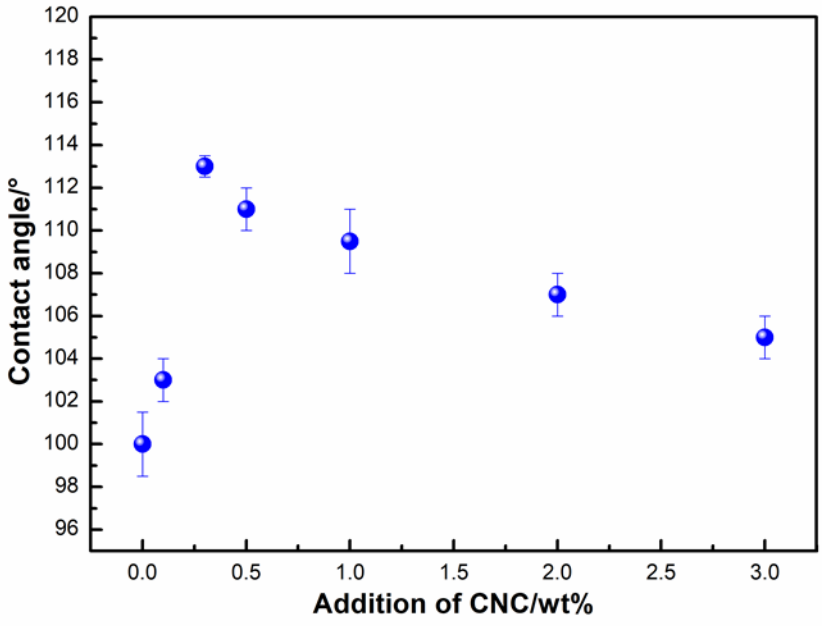

Fig. 7. Contact angle of OACS-based films

All samples had good water resistance with high contact angle (> 90°). The contact angle of films was influenced by the component of OACS. The OACS modified with 0.3 wt% CNC showed the highest DS (0.214), and made the highest contact angle for the film (113°). The contact angle of films increased first and then decreased with the increasing addition of CNC, which had the same trend with DS of OACS. The introduction of CH_3-C=O improved the hydrophobicity of OACS, so high DS led to improved contact angle of composite film. The compact structure of OACS-based film also effectively hindered the permeation of water. The film fabricated by OACS showed a higher contact angle than that found in the films fabricated by CS and OS (33.5° and 66.0°, respectively).

CONCLUSIONS

1. Starch was successfully dual-modified with the assistance of cellulose nanocrystals. The dual-modified starch had a destroyed crystal structure, disrupted morphology, and showed the highest degree of substitution at 0.214.
2. The film fabricated with dual-modified starch, polyvinyl alcohol, and glycerol had a compact structure and showed high transparency, thermal property, tensile strength, and water resistance.
3. This work demonstrated the potential of using CNC as a catalyst in dual-modification of starch and the subsequent starch-based film.

ACKNOWLEDGMENTS

The authors are grateful for the financial support from the National Key Research and Development Program of China (Grant No. 2017YFB0307902), the National Natural Science Foundation of China (Grant No. 31670595, 31770628), the Taishan Scholars Program, and the Higher Educational Science and Technology Program of Shandong Province, China (Grant No. J18KA091).

REFERENCES CITED

Ahmet Alper Aydın, V. I. (2016). "Effect of different polyol-based plasticizers on thermal properties of polyvinyl alcohol (PVOH): Starch blends films," *Carbohydrate Polymers* 1(136), 441-448. DOI: 10.1016/j.carbpol.2015.08.093

Almasi, N. N. B. G. (2016). "Starch–PVOH nanocomposite film incorporated with cellulose nanocrystals and MMT: A comparative study," *International Journal of Food Engineering* 12(1), 37-48. DOI: 10.1515/ijfe-2015-0145

Ashogbon, A. O., and Akintayo, E. T. (2014). "Recent trend in the physical and chemical modification of starches from different botanical sources: A review," *Starch - Stärke* 66(1-2), 41-57. DOI: 10.1002/star.201300106

Aulin, C., Karabulut, E., Tran, A., Wågberg, L., and Lindström, T. (2013). "Transparent nanocellulosic multilayer thin films on polylactic acid with tunable gas barrier properties," *ACS Applied Materials* and *Interfaces* 5(15), 7352-7359. DOI: 10.1021/am401700n

Biduski, B., Silva, F. T. D., Silva, W. M. D., Halal, S. L. D. M., Pinto, V. Z., Dias, A. R. G., and Zavareze, E. D. R. (2017). "Impact of acid and oxidative modifications, single or dual, of sorghum starch on biodegradable films," *Food Chemistry* 214(1), 53-60. DOI: 10.1016/j.foodchem.2016.07.039

Chen, S., Li, F., Li, J., Sun, X., Cui, J., Zhang, C., Wang, L., Xie, Q., and Xu, J. (2018). "Effects of single-modification/cross-modification of starch on the mechanical properties of new biodegradable composites," *RSC Advances* 8(22), 124-1248. DOI: 10.1039/c8ra01592a

Dang, X., Chen, H., Wang, Y., and Shan, Z. (2018). "Freeze-drying of oxidized corn starch: electrochemical synthesis and characterization," *Cellulose* 25(4), 2235-2247. DOI: 10.1007/s10570-018-1701-y

Diop, C., Li, H. L., Xie, B. J., and Shi, J. (2011). "Effects of acetic acid/acetic anhydride ratios on the properties of corn starch acetates," *Food Chemistry* 126(1), 1662-1669. DOI: 10.1016/j.foodchem.2010.12.050

Gutiérrez, T. J., and Alvarez, V. A. (2016). "Properties of native and oxidized corn starch/polystyrene blends under conditions of reactive extrusion using zinc octanoate as a catalyst," *Reactive & Functional Polymers* 112(1), 33-44. DOI: 10.1016/j.reactfunctpolym.2017.01.002

Haafiz, M. K. M., Hassan, A., Zakaria, Z., Inuwa, I. M., Islam, M. S., and Jawaid, M. (2013). "Properties of polylactic acid composites reinforced with oil palm biomass microcrystalline cellulose," *Carbohydrate Polymers* 98(1), 139-145. DOI: 10.1016/j.carbpol.2013.05.069

Halal, S. L. M. E., Colussi, R., Pinto, V. Z., Bartz, J., Radunz, M., Carreño, N. L. V., Dias, A. R. G., and Zavareze, E. D. R. (2015). "Structure, morphology and functionality of acetylated and oxidised barley starches," *Food Chemistry* 168(1), 247-256. DOI: 10.1016/j.foodchem.2014.07.046

Han, F., Liu, M., Gong, H., Lü, S., Ni, B., and Zhang, B. (2012). "Synthesis, characterization and functional properties of low substituted acetylated corn starch," *International Journal of Biological Macromolecules* 50(4), 1026-1034. DOI: 10.1016/j.ijbiomac.2012.02.030

Hong, J., Zeng, X., Buckow, R., and Han, Z. (2018). "Structural, thermodynamic and digestible properties of maize starches esterified by conventional and dual methods: Differentiation of amylose contents," *Food Hydrocolloids* 83, 419-429. DOI: 10.1016/j.foodhyd.2018.05.032

Li, Y., Wang, L., Liang, R., Chen, J., He, X., Chen, R., Liu, W., and Liu, C. (2018). "Dynamic high-pressure microfluidization assisting octenyl succinic anhydride modification of rice starch," *Carbohydrate Polymers* 193(1), 336-342. DOI: 10.1016/j.carbpol.2018.03.103

Lin, Q., Pan, J., Lin, Q., and Liu, Q. (2013). "Microwave synthesis and adsorption performance of a novel crosslinked starch microsphere," *Journal of Hazardous Materials* 263, 517-524. DOI: 10.1016/j.jhazmat.2013.10.004

Liu, Q., Yang, R., Zhang, Z., and Gao, W. (2017). "Improving the cross-linking degree of oxidized potato starch via addition of nanocrystalline cellulose," *Starch - Stärke* 69(11-12), 1700042-1700050. DOI: 10.1002/star.201700042

López, O. V., Lecot, C. J., Zaritzky, N. E., and García, M. A. (2011). "Biodegradable packages development from starch based heat sealable films," *Journal of Food Engineering* 105(2), 254-263. DOI: 10.1016/j.jfoodeng.2011.02.029

Mo, X. Z., Jiang, J. B., Huang, X. M., Yu, F. N., Wu, J. Y., and Huang, S. F. (2014).

"Preparation and characterization of starch acetate/polyvinyl alcohol foams," *Applied Mechanics and Materials* 513-517, 193-196. DOI: 10.4028/www.scientific.net/amm.513-517.193

Pietrzyk, S., Juszczak, L., Fortuna, T., and Ciemniewska, A. (2014). "Effect of the oxidation level of corn starch on its acetylation and physicochemical and rheological properties," *Journal of Food Engineering* 120, 50-56. DOI: 10.1016/j.jfoodeng.2013.07.013

Ravindra, V. Gadhave, P. A. M., and Gadekar, P. T. (2019). "Cross-linking of polyvinyl alcohol/starch blends by epoxy silane for improvement in thermal and mechanical properties," *BioResources* 2(14), 3833-3843. DOI: 10.15376/biores.14.2.3833-3843

Sasiprapa Pitiphatharaworachot, K. C., Sarawood Sungkaew, S. P., and Puangsin, B. (2019). "Starch nanocomposites reinforced with TEMPO-oxidized cellulose nanofibrils derived from bamboo holocellulose," *BioResources* 2(14), 2784-2797. DOI: 10.15376/biores.14.2.2784-2797

Sun, B., Zhang, M., Hou, Q., Liu, R., Wu, T., and Si, C. (2016). "Further characterization of cellulose nanocrystal (CNC) preparation from sulfuric acid hydrolysis of cotton fibers," *Cellulose* 23(1), 439-450. DOI: 10.1007/s10570-015-0803-z

Sun, Y., Gu, J., Tan, H., Zhang, Y., and Huo, P. (2018). "Physicochemical properties of starch adhesives enhanced by esterification modification with dodecenyl succinic anhydride," *International Journal of Biological Macromolecules* 112(1), 1257-1263. DOI: 10.1016/j.ijbiomac.2018.01.222

Surendra Babu, A., Mohan Naik, G. N., James, J., Aboobacker, A. B., Eldhose, A., and Jagan Mohan, R. (2018). "A comparative study on dual modification of banana (*Musa paradisiaca*) starch by microwave irradiation and cross-linking," *Journal of Food Measurement and Characterization* 12(3), 2209-2217. DOI: 10.1007/s11694-018-9837-x

Vigneshwaran, N., Ammayappan, L., and Huang, Q. (2011). "Effect of gum arabic on distribution behavior of nanocellulose fillers in starch film," *Applied Nanoscience* 1(3), 137-142. DOI: 10.1007/s13204-011-0020-5

Xia, Y. Y., Lin, Z. Y., Yang, G. H., Peng, J. M., and Chen, J. C. (2018). "Preparation of nanocrystalline cellulose-NaClO oxidized starch and its application in paper sizing," *China Pulp* and *Paper* 37(11), 12-18. DOI: CNKI:SUN:ZGZZ.0.2018-11-004

Xiao, H., Lin, Q., Liu, G., and Yu, F. (2012). "A comparative study of the characteristics of cross-linked, oxidized and dual-modified rice starches," *Molecules* 17(9), 10946-10957. DOI: 10.3390/molecules170910946

Xu, Z., Li, J., Zhou, H., and Jiang, X. (2016). "Morphological and swelling behavior of cellulose nanofiber (CNF)/poly(vinyl alcohol) (PVOH) hydrogels: Poly(ethylene glycol) (PEG) as porogen," *RSC Advances* 6(49), 43626-43633. DOI: 10.1039/C6RA03620A

Yan, Q., Hou, H., Guo, P., and Dong, H. (2012). "Effects of extrusion and glycerol content on properties of oxidized and acetylated corn starch-based films," *Carbohydrate Polymers* 87(1), 707-712. DOI: 10.1016/j.carbpol.2011.08.048

Yang, W. S., Bian, H. Y., Jiao, L., Wu W. B., Deng, Y. L., and Dai, H. Q. (2017). "High wet-strength, thermally stable and transparent TEMPO-oxidized cellulose nanofibril film via cross-linking with poly-amide epichlorohydrin resin," *RSC Advances* 1(7), 31567-31573. DOI: 10.1039/c7ra05009g

Zamudio-Flores, P. B., Bautista-Banos, S., Salgado-Delgado, R., and Bello-Perez, L. A. (2009). "Effect of oxidation level on the dual modification of banana starch: The

mechanical and barrier properties of its films," *Journal of Applied Polymer Science* 112(1), 822-829. DOI: 10.1002/app.29433

Zamudio-Flores, P. B., Ochoa-Reyes, E., Ornelas-Paz, J. D. J., Aparicio-Saguilán, A., Vargas-Torres, A., Bello-Pérez, L. A., Rubio-Ríos, A., and Cárdenas-Félix, R. G. (2015). "Effect of storage time on physicochemical and textural properties of sausages covered with oxidized banana starch film with and without betalains," *CyTA - Journal of Food* 13(3), 456-463. DOI: 10.1080/19476337.2014.998713

Zavareze, E. D. R., Pinto, V. Z., Klein, B., El Halal, S. L. M., Elias, M. C., Prentice-Hernández, C., and Dias, A. R. G. (2012). "Development of oxidised and heat–moisture treated potato starch film," *Food Chemistry* 132(1), 344-350. DOI: 10.1016/j.foodchem.2011.10.090

Zhao, X. F., Peng, L.-Q., Wang, H.-L., Wang, Y.-B., and Zhang, H. (2017). "Environment-friendly urea-oxidized starch adhesive with zero formaldehyde-emission," *Carbohydrate Polymers* 1(181), 1112-1118. DOI: 10.1016/j.carbpol.2017.11.035

Zhang, L., Xie, W., Zhao, X., Liu, Y., and Gao, W. (2009). "Study on the morphology, crystalline structure and thermal properties of yellow ginger starch acetates with different degrees of substitution," *Thermochimica Acta* 495(1-2), 57-62. DOI: 10.1016/j.tca.2009.05.019

Zhang, Y., Wang, X., Zhao, G., and Wang, Y. (2013). "Influence of oxidized starch on the properties of thermoplastic starch," *Carbohydrate Polymers* 96(1), 358-364. DOI: 10.1016/j.carbpol.2013.03.093

Article submitted: May 9, 2019; Peer-review completed: July 6, 2019; Revised version received and accepted: July 12, 2019; Published: July 17, 2019.
DOI: 10.15376/biores.14.3.7041-7055